An Approach to Map Visibility in The Built Environment from Airborne LiDAR Point Clouds

Zhang, Guan ting; Verbree, Edward; Wang, Xiao jun

DOI
10.1109/ACCESS.2021.3066649

Publication date
2021

Document Version
Final published version

Published in
IEEE Access

IEEE Access
Multidisciplinary | Rapid Review | Open Access Journal

Received January 16, 2021, accepted March 14, 2021, date of publication March 17, 2021, date of current version March 25, 2021.

Digital Object Identifier 10.1109/ACCESS.2021.3066649

An Approach to Map Visibility in the Built Environment From Airborne LiDAR Point Clouds

GUAN-TING ZHANG[1], EDWARD VERBREE[2], AND XIAO-JUN WANG[1]

[1]Department of Landscape Architecture, School of Architecture, Southeast University, Nanjing 210096, China
[2]Department of Architectural Engineering and Technology, Faculty of Architecture and the Built Environment, Delft University of Technology, 2628 BL Delft, The Netherlands

Corresponding author: Xiao-Jun Wang (xjworking@163.com)

This work was supported in part by the National Nature Science Foundation of China under Grant 51878144 and Grant 50978054.

ABSTRACT Sustainable development can only be achieved with an innovative improvement from the way we currently analyze, design, build and manage our urban spaces. Current digital analysis and design methods for cities, such as visibility analysis, deeply rely on mapping and modeling techniques. However, most methods fall short of depicting the real visual landscape in the urban realm and this could bring a significant error in visibility calculations which may lead to an improper decision for urban spaces. The technical development of light detection and ranging(LiDAR) technology introduces new approaches for urban study. LiDAR utilizes point clouds including thousands or even millions of georeferenced points, and thus can support 3-D digital representation of urban landscape with detailed information and high resolution. Besides the superiority in representing urban landscape, LiDAR point clouds also has a clear advantage in quantitative analysis and provides better visibility than traditional models. In this paper, we first introduced a novel approach to map visibility in the urban built environment involving vegetation data directly using airborne LiDAR point clouds. This approach calculates neighborhood statistics for occlusion detection. Then we presented 2 case with different scenarios showing how our approach can be used to obtain a precise visibility in an urban area in the Netherlands. At last, we discussed how point clouds based visibility models can be further explored and can better assist urban design.

INDEX TERMS Visibility analysis, airborne LiDAR, urban area, built environment, point cloud, visual environment.

I. INTRODUCTION

Urbanization is increasing across the globe, with recent UN statistics confirming that more than half the world's population live in urban areas [1]. More than two-thirds of the world's population will live in urban areas by 2050. While many benefits from efficient and modern cities are well understood, this rapid urbanization also risks urban sustainability. One risks is devastation of city images. With rapid urbanization, particularly in China, mushrooming high-rise buildings haven't been well organized or planned in urban spaces. This has severely deteriorated city visual environments, mostly due to poor visual management. If we wish to shape an visually enjoyable urban landscape, it is important for designers and administrators to understand how the physical aspects of a landscape, such as the visual properties, are perceived. A good visual management could be based on results of a reliable quantitative visual analysis which can reveal current visual issues in an urban space.

Visibility analysis for urban spaces is a fundamental process for building or protecting city images [2]–[5]. Several previous studies have established that 90% of transmitted information in the human brain is from visualization, hence we feel the world through our eyes. Consequently, urban visual environments are crucial for people to know a city. Reliable visibility results can help planning or managerial decision making for better visual environments [6]. Well-designed visual environments can help citizens to be happy and relaxed in their daily life and can also help create a sustainable city. However, it remains challenging for urban management to depict visual implications due to increasingly complicated urban environments.

Geographic information systems (GISs) have become common tools to explore human visual space [7]–[10].

The associate editor coordinating the review of this manuscript and approving it for publication was Leonel Sousa.

However, most modern GIS based visual analyses have limitations in urban spaces. Most GISs are based on two (2-D) or 2.5 (2.5-D) dimensional models [11]–[13], which tend to only poorly represent real urban space details, whereas accurate visibility models require extremely detailed spatial information for urban three-dimensional (3-D) objects. Light detection and ranging (LiDAR) point cloud data offers opportunities to compensate for disadvantages associated with from traditional analyses [14], [15].

LiDAR technology has investigated for decades, with many studies in archaeology [16], [17], construction [18], visualisation [19]–[21], etc. However, employing LiDAR point clouds for urban space visibility analyses is a new and rapidly developing research area worldwide. Compared to visualisation research which focuses on rendering a emulated world in a digital way, visibility analyses aim at finding visible areas from a single or multiple observation points. Point cloud data offers several benefits for visibility analysis, and could be much more flexible and efficient than previous models.

- Mapping visibility directly from point clouds can skip the process of generating surface object/vector or grid/raster representation models. They can be employed directly for visibility analysis, significantly reducing analysis time and computational requirements.
- Point cloud data generally has high density and high accuracy, commonly more than 10 points/m^2 up to 1000 points/m^2. This allows precise and accurate data usage for visualisation and analysis, with significantly improved visibility analysis.
- Traditional surface models neglect vegetation due to difficulty representing trees or shrubs, etc. However, tree and related impact on visibility analysis cannot be ignored, particularly in summer time when trees can partially block lines-of-sight (LoSs). Point cloud data provide considerably more detailed information than traditional raster data or digital elevation model (DEM), hence it is much easier to represent and analyse vegetation effects.
- Point clouds can be organized in different levels of details (LoDs), which can considerably improve analysis execution speed [22], [23].

The four most common techniques for LiDAR visibility analyses include surfaced based, voxel based, hidden point removal, and ray-tracing approaches [24], and their application have been well studied for many scenarios. Some applications focused on natural environments [25]–[27] or suburban areas [28] with few or no artificial constructs. Several discussed the visibility in built environments [29], but neglected visual impacts from urban vegetation. Generally, only one observation point within any test site was analysed. Thus, visibility for built environments considering both buildings and vegetation using point clouds with multiple observers requires further discussion and research.

In our previous study [14], we generated a solid cube for each point to represent the visual obstruction. The data we used is a mobile point cloud. The process of cube generation is really time consuming. And the approach extremely depends on the integrity and consistency of the input data, a mobile point cloud has a defect that upper parts of urban objects are not complete, this would result in unreliability and inaccuracy. Conversely, in airborne point clouds, the roof information is relatively complete, but the density of facade points is too low to block the line of sight. However, we can still distinguish the space occupied by buildings through the rooftop information [20].

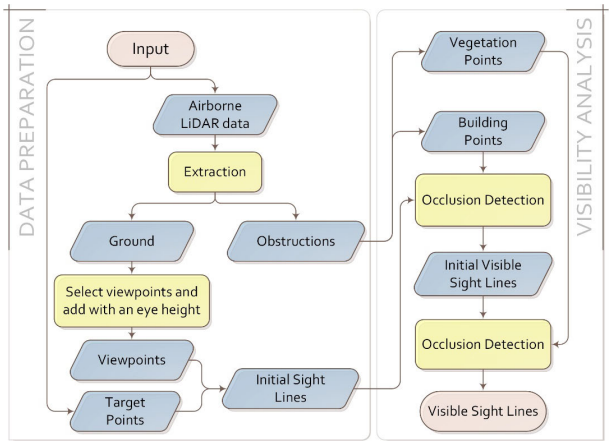

FIGURE 1. Proposed visibility analysis method workflow.

Therefore, we propose a visibility analysis approach employing occlusion detection with airborne LiDAR point clouds to thoroughly analyse urban space visibility considering both buildings and vegetation. What we are interested is the intervisibility between observers and target landscapes in a digital urban area represented by massive points. The intervisibility reveals that if an observe can see the target. This paper provides a brief review of recent visibility analysis studies (part 1) and introduces the proposed point cloud based visibility analysis methodology (part II). We then analyse 2 relevant cases (part III and part IV), and finally summarize and conclude the paper with some suggestions for future work (part V).

II. METHODOLOGY

This paper introduces a point cloud based method offering a comprehensive visibility result for urban planning and urban design, as shown in FIGURE 1. Proposed visibility analysis method workflow. A viewpoint is defined as the location where observers see from. A target point represents an object which plays a significant role in the urban visual environment. This object can be a building with histories considered as a feature in the city, and it should be more exposure in urban spaces to promote the city image.

A. DATA PREPARATION

Airborne LiDAR point clouds should be well classified into ground, buildings, vegetation, and other points. Building and vegetation points are extracted as obstructions for visibility analysis. This study considered the view from pedestrians, hence viewpoints were extracted from ground points with

a proper distance to reduce the calculation time and added with eye height. A target was a specific feature in the study area, which was considered to be a featured landscape to improve or preserve the current urban image. For quantitative analysis, targets were discretized into points. Initial sight lines were straight lines comprised two vertices representing the viewpoint and target point to which visibility was determined.

B. OCCLUSION DETECTION FOR CALCULATING VISIBILITY

We created a set of search points derived from LoSs between viewpoints and target points, and used sight lines with certain increments to track along the LoS and detect occlusions.

Airborne LiDAR point cloud data were the base information for the proposed approach, but building details are poorly collected from airborne sensors. Only roofs, vegetation, and ground are well presented in airborne point clouds, whereas building and vegetation complexities are quite different for obstructions for visibility analysis.

Therefore, we propose two strategies for building and vegetation occlusion detection. The main occlusion detection concept is to detect obstacle point densities in a given area. If obstacle point density exceeds some threshold, then this area can be considered occlusive, i.e., LoSs cannot pass through this area.

1) STRATEGY FOR BUILDING POINTS

Building roof information is relatively complete in airborne LiDAR point clouds, but facade point densities are generally too low to block LoS. However, we can still distinguish space occupied by buildings using rooftop information [20]. Since there are insufficient side points (see FIGURE 2), we assumed that if there were sufficient rooftop points above a certain space, this space was occupied by a building. Space under rooftop points were considered as LoS obstacles.

Suppose there are a point cloud of building rooftops and a set of search points generated along an LoS between a viewpoint and a target point. First, we find building points above the current search point, which are considered as obstacle candidates. Occlusion detection for building points entails counting the number of candidate obstacle points surrounding a search point on the XY plane(see FIGURE 3). If this number exceeds a threshold, then this LoS is blocked and is marked as invisible.

2) STRATEGY FOR VEGETATION POINTS

In contrast, vegetation is relatively complete in airborne LiDAR point clouds, with tree crowns and trunks generally well presented. Thus, vegetation points are sufficiently detailed to directly conduct occlusion detection. A 3D detection sphere is generated for each search point and LoS visibility calculated according to the number of points inside the sphere. If sufficient points occur within any detective sphere whose centre is an LoS search point, the sphere is classified as occlusive (see FIGURE 4), and the LoS is marked as invisible.

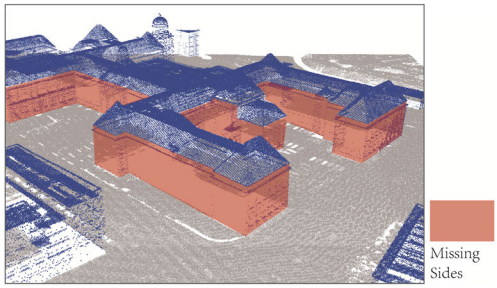

FIGURE 2. Typical missing building side points from an airborne LiDAR point cloud.

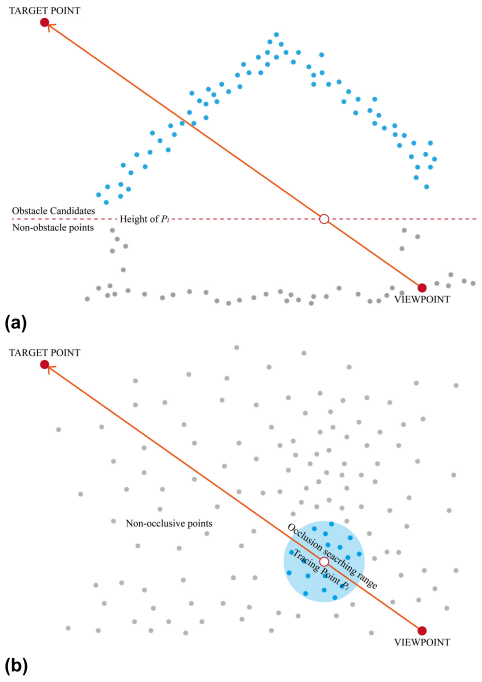

FIGURE 3. Proposed occlusion detection strategy for building points: (a) selecting obstacle candidates from identified building points, (b) searching along the sight line to detect occlusions in the XY plane.

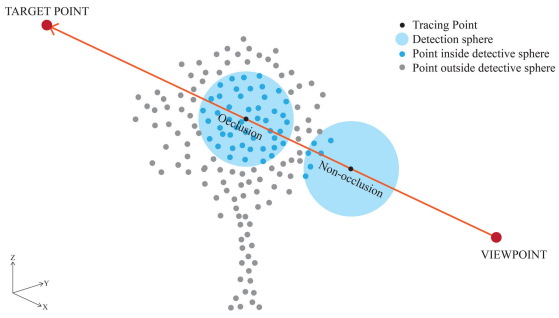

FIGURE 4. Proposed occlusion detection strategy for vegetation points.

C. ALGORITHMIC STEPS OF VISIBILITY ANALYSIS

We implement the proposed algorithm in Python. FIGURE 5 shows the analysis process assuming a line of sight LoS, building point cloud P_B, and vegetation point cloud P_v. The corresponding algorithmic steps are as follows.

(1) Create a set of searching points $P_S \in LoS$, the creation is according to the value of search range r_0, the number of P_S equals to l_{LoS}/r_0, where l_{LoS} is the length of current LoS;
(2) For each search point $p_i \in P_S$, perform following steps from the viewpoint:
   a) set up an empty list of obstacle candidates O_C;
   b) find obstacle candidate building points with $z > z(p_i)$ (FIGURE 3(a)), and save candidates to O_C;
   c) create a k-D tree representation T_B for XY coordinates of O_C, then count T_B neighbours to identify the number of candidates within radius r_0 around p_i, record this number as n_i;
   d) if $n_i > n_0$, the algorithm terminates and LoS is coded as 0 and marked as invisible; if $n_i < n_0$, then $i = i + 1$, and repeat step 2 until the detection circle of the last search point (i.e., the target point) is identified as not occlusive, hence LoS is determined to be visible and coded as 1;
(3) if LoS is coded as 1 in step 2, create a k-D tree representation T_v for P_v;
(4) For each search point $p_j \in P_S$, perform following steps from the viewpoint:
   a) count neighbours for T_v to identify occlusion candidates within radius r_0 around p_i, record this number as m_i;
   b) if $m_j > m_0$, the algorithm terminates and LoS is recoded as 0 and marked as invisible; if $m_j < m_0$, then $j = j + 1$, and repeat step 4 until the detection circle of last searching point (i.e., the target point) is identified as not occlusive, hence LoS is determined to be visible and the value remains 1;

As discussed above, the number of points within a search range around a search point p_i is considered for judging occlusion. If the number exceeds some threshold depending on the point cloud density, the search point is considered to be inside a building, i.e., occluded. Consequently, the corresponding LoS is marked as invisible and visibility analysis stops for that LoS. In contrast, if the number fails to reach the threshold, the search range around p_i is considered as non-occlusion and analysis continue to the next point p_{i+1}. Time complexity of the algorithm is O(n2logn), where 'n' represents the number of input LiDAR points.

D. CUMULATIVE VISIBILITY

We propose a vector based analysis called cumulative visibility, based on the cumulative viewshed concept [30]. In contrast with raster based cumulative viewshed, cumulative visibility is derived from vector sight lines. Hence the result for each discrete visibility calculation is either positive or negative, conventionally coded as 1 or 0 for visible or invisible LoS, respectively. Viewpoints for a visible LoS are also coded as 1. Thus, the maximum visibility value for a visible viewpoint = 1 if there is only one target point, but a viewpoint may see more than one target point if there are multiple target points. Thus, cumulative visibility for a viewpoint measures how many target points can be seen from the viewpoint.

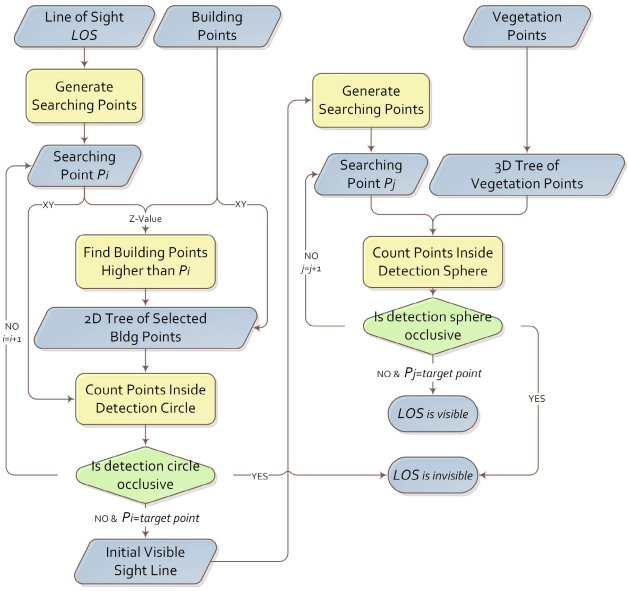

FIGURE 5. Workflow for the proposed visibility analysis algorithm.

III. MATERIALS

A. EXPERIMENTAL STUDY AREAS

Two cases are selected for testing our proposed analysis to see if the algorithm is effective in different urban morphologies. Case 1 and Case 2 belong to Delft and Rotterdam, the Netherlands respectively.

Case 1 is a small area of the Delft University of Technology (located in Delft, The Netherlands) was chosen as the study area, in particular the tower dome for the Bouwkunde (BK, Faculty of Architecture and the Built Environment) building. Buildings in case 1 are multi-storeyed, the average height of buildings within is about 20m.The dome has a beautiful shape and high volume, and can be seen from large distances in the surrounding urban areas, since its elevation ≈28.5 m.

Case 2 is located in an urban area around the Rotterdam Centraal railway station which is the main railway station of the city Rotterdam in South Holland, Netherlands. There are several high-rise buildings located in this area. The average height of buildings within is about 50m. The building of Houthoff Rotterdam is considered as the target in our analysis. The building top's elevation is 110m.

FIGURE 6 shows two experimental study areas and FIGURE 7 illustrates the viewing target in two cases.

B. INPUT POINT CLOUDS

The origin airborne LiDAR data of both 2 cases was downloaded from AHN3 (ref: www.ahn.nl, see FIGURE 8). As a mature product, the AHN point cloud is well classified into ground, building, vegetation, etc., the procedure of classification combines with automatic and manual manners [31]. Then we could easily extract points in the different classifications.

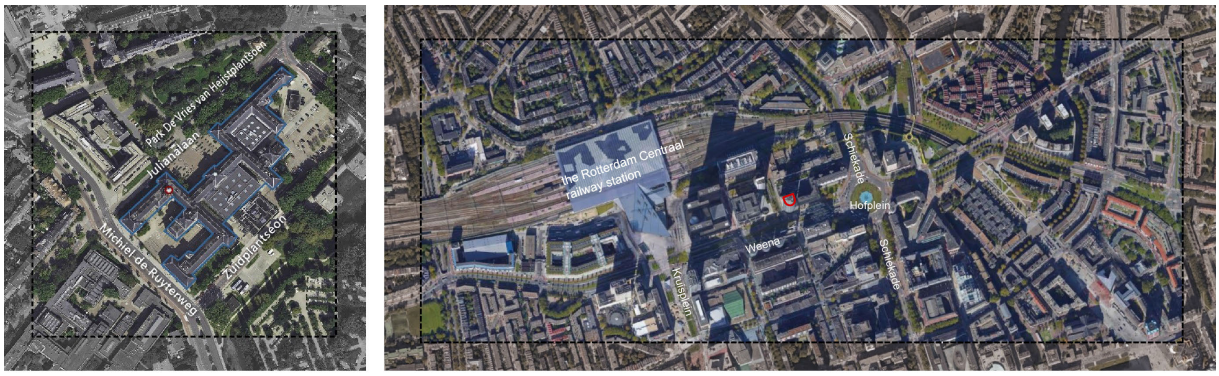

FIGURE 6. Top views of experimental study areas to implement the proposed analysis (downloaded from Google maps).

(a) Case 1 (taken by the author)

(b) Case 2 (from Google)

FIGURE 7. Street view of two cases with the selected target outlined in red.

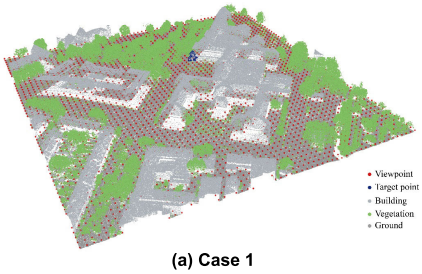

(a) Case 1

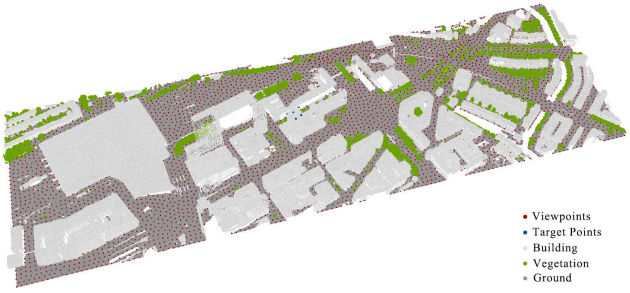

(b) Case 2

FIGURE 8. Input data for the proposed analysis case study.

TABLE 1. Classifications of original point cloud.

Study Case	Category	Ground	Vegetation	Buildings	Water	Whole Dataset
CASE 1	Number of points	1,074,195	529,167	978,238	39	2,581,639
	H_{max}(m)	1.555	28.495	52.911	-	52.911
	H_{min}(m)	-3.346	-1.706	-0.313	-	-3.346
CASE 2	Number of points	4,171,535	1,571,307	3,400,560	-	9,143,402
	H_{max}(m)	4.648	46.534	153.644	-	52.911
	H_{min}(m)	-6.323	-2.471	-5.829	-	-3.346

* H_{max} means the highest elevation, H_{min} means the lowest elevation.

The area of case 1 is 300 × 300 m, and the area of case 2 is 1400 × 450 m. Both are small areas with numerous points. There are 2,581,639 points in the original point cloud of case 1 and 9,143,402 points of case 2, Table 1 shows the number of points in each category. Ground points are used to generate viewpoints, but the original ground points were too dense and redundant. We reduced the ground points randomly to 5 m minimum for case 1 and 10 m minimum for case 2, and added an extra-height to these points. Target points are evenly extracted from the surface of the dome such that every target point had an equal chance to be seen. The total number of viewpoints, number of targets and number of construct lines between viewpoints and targets in different cases can be found in Table 2. FIGURE 8 shows the input data distribution.

FIGURE 9 compares point cloud models with and without vegetation to evaluate visual impacts from vegetation in urban areas. Model 1and Model 3 contain building points only, Model 2 and Model 4 contains building and vegetation points.

TABLE 2. Number of viewpoints, target points and construct lines.

Study Case	Number of Viewpoints (N_V)	Number of Target Points (N_T)	Number of Construct Lines between Viewpoints and Target Points ($N_V \times N_T$)
CASE 1	3,184	40	127,360
CASE 2	4,304	5	21,520

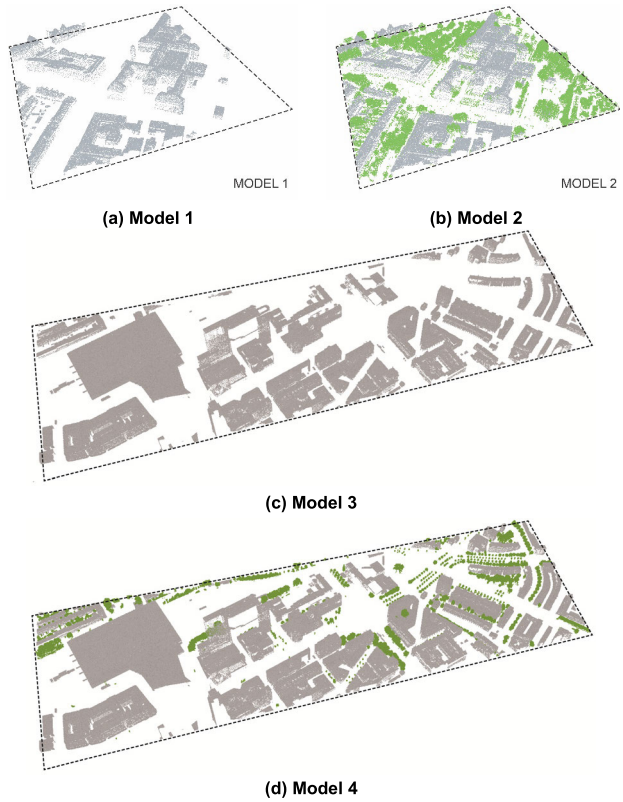

FIGURE 9. Comparison point cloud models including (a) and (c)building points only; (b) and (d) building and vegetation points.

C. PARAMETER DETERMINATION

1) EYE HEIGHT FOR VIEWPOINTS

Since we considered public spaces within the city, ground points (outdoor space) were used to generate viewpoints. Ground points have been downsized by enlarging average point spacing to 5 m in case 1 and 10 m in case 2. Then we added height of 1.6 m as average eye level.

2) SEARCH RANGE

Since the resolution of input data of two cases is the same, we used case 1 to discuss the proper parameters for visibility analyses.

The search range r_0 should not be too large or too small for analysis. If the range is too large, there may be too much noise; and if too small, there may be insufficient obstruction points inside the search range for occlusion detection. Thus, r_0 should be a reasonable value to obtain an accurate and reliable result.

Human eyes can distinguish an 0.3 m diameter object up to maximum 1 km distance [32]. This study had longest sight line between viewpoint and target ≈225 m in case 1 and 740 m in case 2, i.e., considerably less than 1 km. FIGURE 10 shows demonstration results from a solid model for several r_0 around 0.15 m to identify an optimal r_0 for this case. Point cloud with $r_0 = 0.15$ m was closest to the demonstration model. Thus, search range with diameter 0.3 m (i.e.., $r_0 = 0.15$ m) was a suitable choice for both 2 cases.

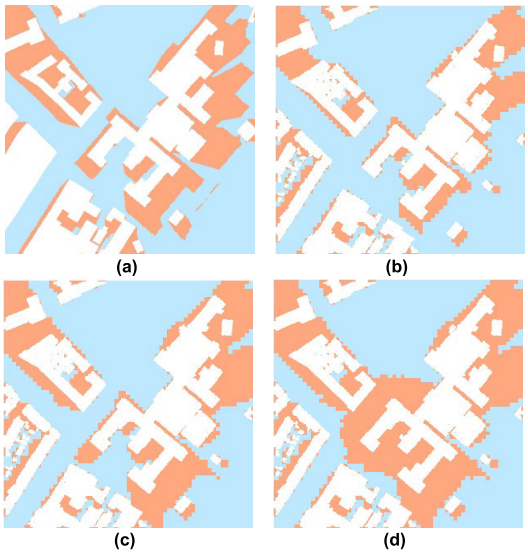

FIGURE 10. Visibility maps of case 1: (a) demonstration solid model; and building point clouds with (b) $r_0 = 0.10$ m, $n_0 = 11$; (c) $r_0 = 0.15$ m, $n_0 = 14$; and (d) $r_0 = 0.25$ m, $n_0 = 15$. Red and blue represent invisible and visible areas, respectively.

3) OCCLUSION THRESHOLD

The threshold to identify a occlusive search range should be assigned based on point density. CloudCompare v2.6.3, a 3D point cloud processing software [33], is used to calculate obstruction point density, with average building point surface density ≈14.2 points/πr_0^2. Therefore, we set building point occlusion threshold $n_0 = 14$. Similarly, average vegetation point density = 18 points/πr_0^3 and hence vegetation point occlusion threshold $m_0 = 18$.

IV. RESULTS

A. CASE 1: MULTI-STOREYS BUILDINGS

1) VISIBILITY MAP

FIGURE 11 shows the proposed visibility analysis implemented for models 1 and 2 (see figure 8) and visualized on ArcGIS Desktop [34]. The algorithm implemented for model 1 and model 2 had differences on steps according to the classification of input points. Steps 1 and 2 were applied to model 1, whereas all algorithmic steps (i.e., steps 1–4) were run on model 2. Visible areas in model 2 (576) shrunk dramatically compared with model 1 (1676) due to vegetation effects, i.e., only approximately one-third of visible areas from model 1 remained visible in model 2 (see FIGURE 11).

2) OVERLAPPED VISIBILITY MAPS

FIGURE 12 shows the visible points for the two visibility maps from FIGURE 11 overlapped. Most model 1

TABLE 3. Visibility statistics for the proposed approach on Models 1 and 2 (see FIGURE 9).

	Number of visible viewpoints (N_{VV})	$\frac{N_{VV}}{N_V*}$	Cumulative visibility		
			Maximum	Minimum	Mean
Model 1	1676	52.64%	20	1	13.17
Model 2	576	18.09%	20	1	9.79

* Number of total input viewpoints in Case 1, $N_V = 3184$.

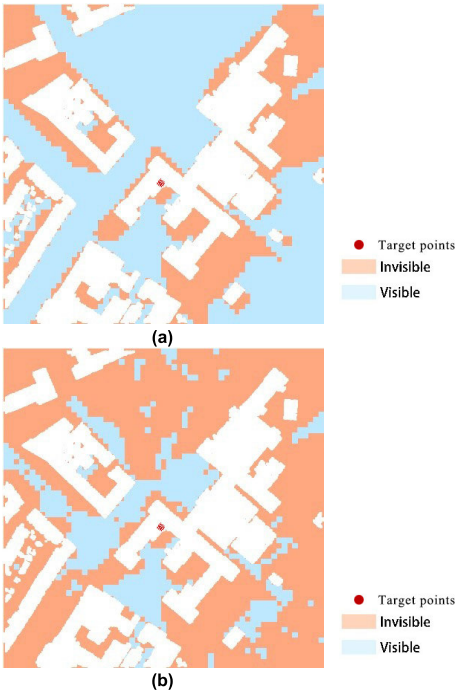

FIGURE 11. Visibility maps of case 1 from the proposed analysis method for (a) model 1 and (b) model 2 (see Figure 8).

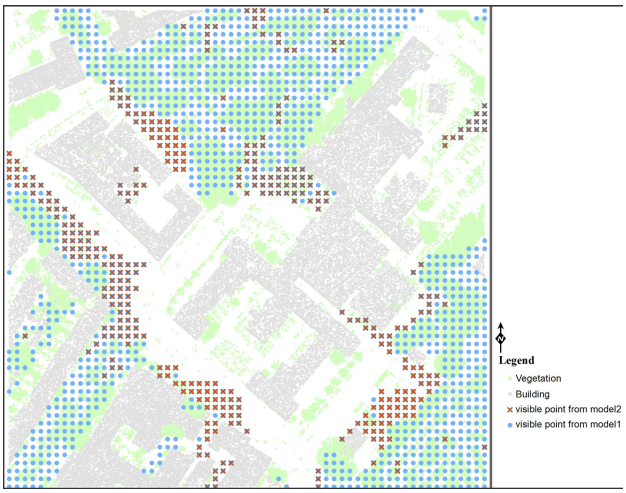

FIGURE 12. Overlapped visibility maps of case 1 from Figure 11 (visible points only).

visible points occurring inside areas covered by vegetation are marked as invisible in model 2. De Vries van Heijst-plantsoen Park can be a good location to enjoy the view

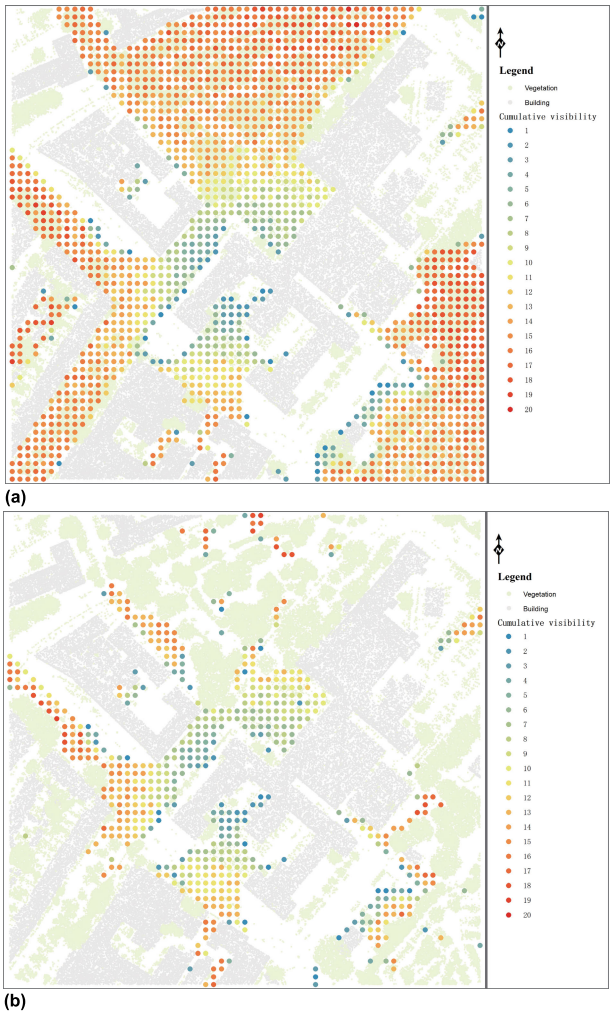

FIGURE 13. Cumulative visibility maps of case 1 for (a) model 1 and (b) model 2 (see Figure 8).

of our target landscape if there are no trees inside. When considering vegetation in model 2, lush green vegetation in the park has become the most obstruction of vision. As a result, we can hardly see the dome from the park. Due to the road greening has blocked the sight lines, model 2 points are relatively concentrated close to buildings, whereas model 1 visible points have a spread distribution.

3) CUMULATIVE VISIBILITY

FIGURE 13 shows cumulative visibility for models 1 and 2, with corresponding statistics in Table 4. Maximum for both models = 20, i.e., half the target points. Thus, a single viewpoint can see no more than half the dome at any time. FIGURE 13 (a) shows that model 1 viewpoints close to the tower did not achieve high cumulative visibility, high cumulative visibility points are located in areas far from the tower. Thus, viewing from larger distance achieved better target view, consistent with the D/H ratio proposed by Tao and Qing [35]. The cumulative visibility of visible viewpoints in FIGURE 13(b) shows that model 2 is not significantly

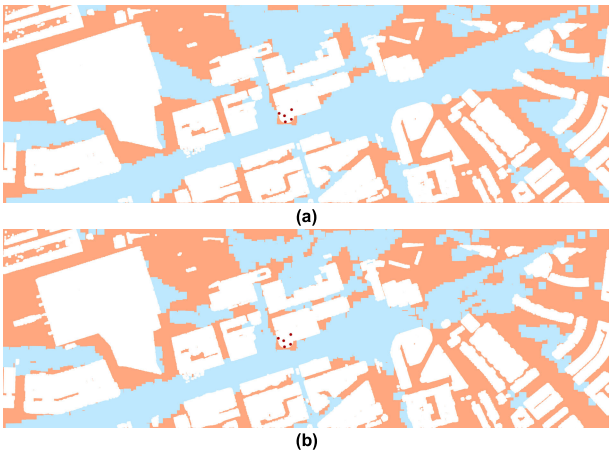

FIGURE 14. Visibility maps of case 2 from the proposed analysis method for (a) model 3 and (b) model 4 (see Figure 8).

different regarding distance viewing. Thus, vegetation doesn't make a significant difference to the value of cumulative visibility. Figure 13(b) also shows that the best viewing location is two streets named Michiel de Ruyterweg and Julianalaan respectively and also two plazas belonging to the BK building. These two streets are both located to the west of the building (see FIGURE 6(a)).

B. CASE 2: HIGH-RISE BUILDINGS

1) VISIBILITY MAP

The process of analysing case 2 is identical to case 1. Steps 1 and 2 of proposed algorithm described in part II were applied to model 3, whereas all algorithmic steps were run on model 4. FIGURE 14. Visibility maps of case 2 from the proposed analysis method for (a) model 3 and (b) model 4 (see Figure shows visibility results of case 2. Because the target is high enough to be seen, the selected building top is highly visible within study areas from ground level. There are continuous visible areas along Weena Street in both model 3 and model 4, it means that people can enjoy a good view of the building top from this street. Visible areas in the model with vegetation haven't drop obviously compared to the model with only building points. The change of visible areas of case 2 is quite different from the situation of case 1. The difference contributes to the different vegetation conditions. Trees in case 1 are much more abundant in case 2, as a result, trees have a great impact on the visibility result in case 1.

2) OVERLAPPED VISIBILITY MAPS

FIGURE 15 shows the visible points for the two visibility maps from FIGURE 14. The result shows that 334 model 3 visible points occurring inside areas covered by vegetation are marked as invisible in model 4, the decreasing number of visible points in case 2 is much less than case 1. Because of sparse vegetation along the west side of Weena Road, there is a very subtle change of visible areas within these road sections.

TABLE 4. Visibility statistics for the proposed approach on Models 1 and 2 (see Figure 8).

	Number of visible viewpoints (N_{VV})	$\frac{N_{VV}}{N_V *}$	Cumulative visibility		
			Maximum	Minimum	Mean
Model 1	1613	37.48%	4	1	2.26
Model 2	1279	29.72%	4	1	2.18

* Number of total input viewpoints in case 2, $\boldsymbol{N_V = 4304}$.

3) CUMULATIVE VISIBILITY

FIGURE 16 shows cumulative visibility for models 3 and 4, with corresponding statistics in Table 4. The table indicates that maximum for both models $= 4$. FIGURE16(a) shows that viewpoints close to the building did not achieve high cumulative visibility. Viewpoints with high cumulative visibility are mostly located in the west side of Weena Road, where is quite far from the target building. This situation is very similar to case 1. Also, the approximate distributions of cumulative visibility of model 3 and model 4 indicates that vegetation indeed can't effect the cumulative visibility evidently.

V. DISCUSSION

A. VEGETATION IMPACT FOR VISIBILITY ANALYSIS

The case study verified that vegetation in urban spaces can have a dominant impact for visibility analysis when the viewpoint is selected from ground, creating significant obstruction between observers and enjoyable landscapes in very green environments. The result of cases with different urban scenarios reveals sidewalk planting could be the biggest visual obstacles.

Therefore, traditional visibility analyses that only consider buildings could fail to represent real visibility. Since vegetation has become a crucial element in modern urban spaces, including vegetation in visibility analysis will help obtain reliable visibility maps. The proposed approach improves visibility map accuracy by explicitly considering vegetation in contrast with traditional viewshed or visibility analysis that neglects vegetation.

B. THE PROPOSED VISIBILITY ANALYSIS ACCURACY

Figure 13 shows typical pictures for viewpoints at the indicated locations. Point cloud models with vegetation were quite reliable compared with empirical views, providing visibility close to the real case. Thus, the proposed visibility analysis approach using LiDAR point clouds to obtain detailed and reliable results without modeling provides realistic visibility maps.

C. POTENTIAL APPLICABILITY FOR URBAN DESIGN

There are many potential applications for LiDAR point cloud based visibility analysis in urban design. Accurate quantitative visibility maps will be very useful for many purposes, e.g. cumulative visibility analysis can help to identify optimal location(s) to enjoy landmarks or enjoyable sites, and space between viewing locations and landmarks could be

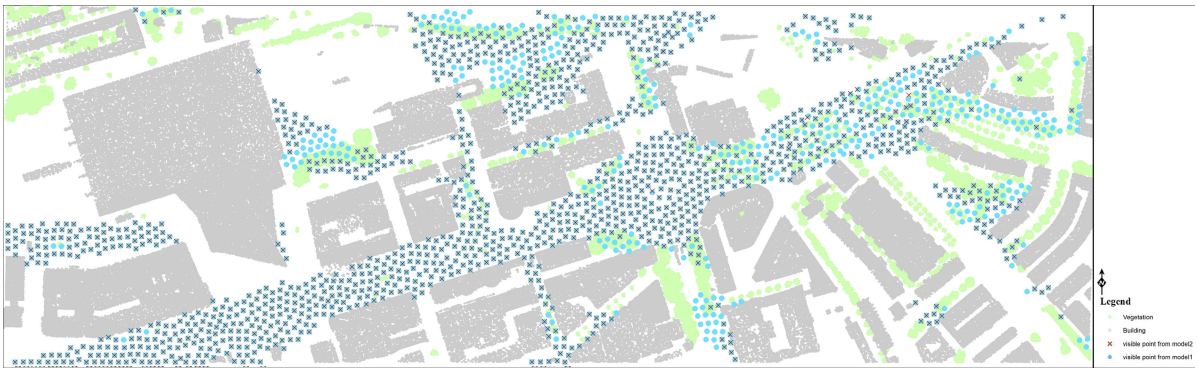

FIGURE 15. Overlapped visibility maps of case 2 from Figure 14 (visible points only).

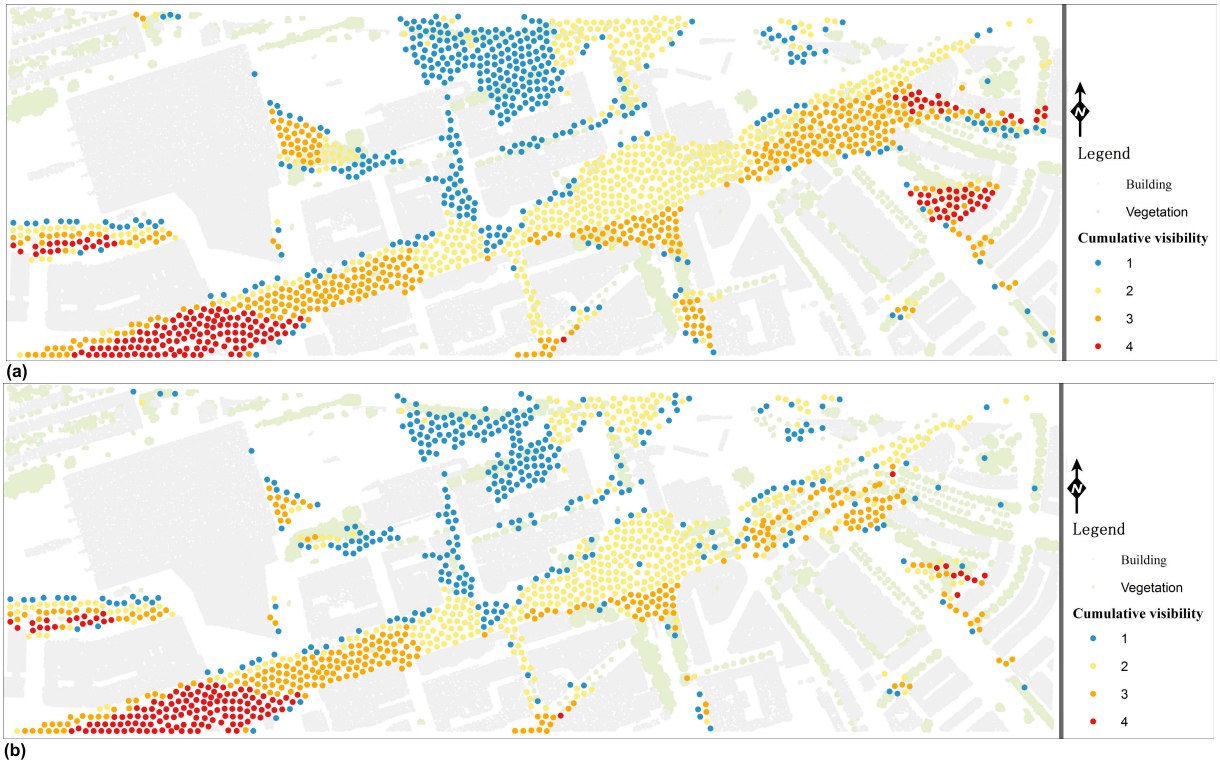

FIGURE 16. Cumulative visibility maps of case 2 for (a) model 3 and (b) model 4 (see Figure 8).

reasonably controlled to protect the view. The proposed analysis can also provide major indicators to enrich urban space quality by subsequently assessing view based environmental enhancement.

Blue points in our results (see FIGURE 17) can be considered as suitable viewpoints to enjoy a better view of the dome. Thus, spaces between those viewpoints and the dome could be controlled to preserve the current view. Yellow points are invisible viewpoints due to vegetation. Some of these viewpoints could become visible if the trees were well trimmed or sensibly removed. Red points are blocked by buildings, which would normally leave little opportunity to improve visibility, but such changes could be considered in cases where building changes are already proposed (e.g. removing an old building and replacing with differently shaped building).

From the result, we can see that vegetation plays a significant role in urban visual environments, especially in a green environment with narrow roads. Trees could be a huge obstacle between observers and beautiful landscapes, to deal with this kind of situation, trees might be removed carefully by the authority according to a reliable visibility result. But in a different scenario, if there is a visually unpleasant object inside an urban area, trees can be a perfect cover for this. Overall, trees could be positive or negative in urban visual landscape. A visibility analysis considering vegetation can

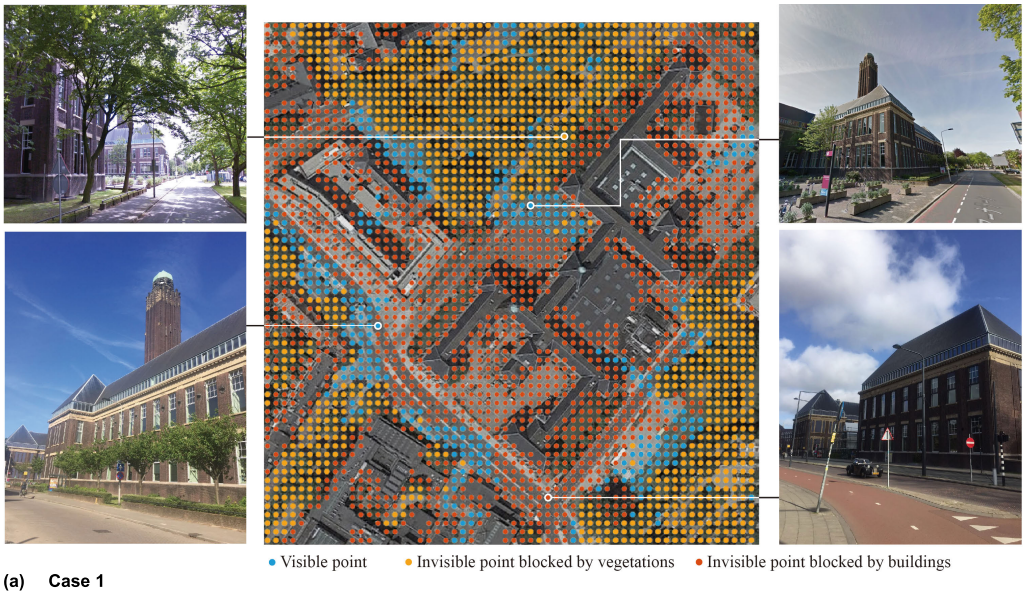

(a) Case 1

(b) Case 2 (photos downloaded from Google)

FIGURE 17. Visibility map for case 1 and case 2 as well as some typical viewpoint photos.

help us to quantify the visual impact of vegetation in urban environments, and the quantitative results are considerably helpful for rationally shaping a city with a pleasant visual landscapes.

D. THE USE OF K-D TREES

We used k-d trees to reduce execution time to re-construct point cloud data for occlusion detection, achieving computation times a small as 155 fold less than previously. Thus,

the system required only 0.2–0.5 s to computing visibility for a single LoS. The Python based Scipy ecosystem of open-source software was used to construct k-d trees and for range searching.

E. LIMITATIONS

Although the proposed point cloud based visibility analysis improves visibility map quality, it also requires a significantly large and well classified dataset for analysis. For the analysis of Vegetation blockage should also consider a strategy to represent vegetation semi-transparency. Even a leafy tree fails to entirely block LoSs, and seasonal differences should also be considered. Thus, it is inaccurate to simply define sight lines passing through trees as just visible or invisible, intermediate state(s) should be considered.

All computations were conducted on a consumer level PC with Intel®Core i7 3.19 GHz CPU, 16 GB RAM, and Windows®10, 64 bit operating system. Total time to calculate visibility for model 2 = 892 minutes (127,360 construct lines with 1.5 million points) and for model 3 = 1024 minutes (20,655 construct lines with 5 million points). Although implementing the k-d tree algorithm in Python significantly improved computation efficiency, it remains too large, particularly if a whole urban area needed visibility analysis. Increased input data complexity and size may mean days or even weeks to calculate using the current algorithm.

VI. CONCLUSION

Quantitative 3D visual space analysis is critical to understanding urban built environment visual characteristics. This study proposed an airborne LiDAR point cloud based visibility analysis approach to not only quantify visibility in urban space but also measure visual impacts from vegetation. The main concept for the proposed visibility analysis is to detect occlusion along sight lines between the viewpoint and target. We also proposed cumulative analysis to find viewing locations that provide better target views. We implemented the proposed approach for two cases with different urban areas to verify the approach and highlight advantages. Results showed that our algorithm is available for both urban scenarios with multi-storey buildings and high-rise buildings, in another word, our algorithm has the potential for widespread use.

The proposed analysis more effectively simulated real spatial visibility compared with traditional analyses that generally neglect vegetation impacts. Mapping cumulative visibility distribution identified and quantified visual characteristics for any location in urban spaces. The analytical and visualized result could help to better understand urban morphology and provides a reliable reference for urban planning or design decision making.

There were several limitations in the proposed analysis. Future research will apply the proposed approach to a more complex urban environment, identifying visual properties for large scale urban spaces and essential features behind the urban form. Also, we will alter the type of targets and viewpoints in future case study, for instance, visibility between two buildings from upper floor level. The approach should extend vegetation treatment to non-binary states (i.e., partial visibility), and include buildings with underpasses or tilted walls and bridges. Faster data processing should be investigated through reducing data redundancy. Well-organized point clouds and levels of detail (LoDs) will help filtering irrelevant information from the analysis.

ACKNOWLEDGMENT

The authors would like to thank prof.dr.ir. P.J.M. van Oosterom for preliminary research support, as well as the valuable comments from Dr. Ming-xue Zheng and Dr. Xin Li.

REFERENCES

[1] *World Urbanization Prospects: The 2019 Revision*, Dept. Econ. Social Affairs, New York, NY, USA, 2019.
[2] D. Fisher-Gewirtzman and I. A. Wagner, "The spatial openness index: An automated model for three-dimensional visual analysis of urban environments," (in English), *J. Architectural Planning Res.*, vol. 23, no. 1, pp. 77–89, 2006. [Online]. Available: https://WOS:000236713100005
[3] W. C. Malm, B. Schichtel, J. Molenar, A. Prenni, and M. Peters, "Which visibility indicators best represent a population's preference for a level of visual air quality?" (in English), *J. Air Waste Manage. Assoc.*, vol. 69, no. 2, pp. 145–161, Feb. 2019, doi: 10.1080/10962247.2018.1506370.
[4] Y. Zheng, S. Lan, W. Y. Chen, X. Chen, X. Xu, Y. Chen, and J. Dong, "Visual sensitivity versus ecological sensitivity: An application of GIS in urban forest park planning," *Urban Forestry Urban Greening*, vol. 41, pp. 139–149, May 2019, doi: 10.1016/j.ufug.2019.03.010.
[5] S. Yu, B. Yu, W. Song, B. Wu, J. Zhou, Y. Huang, J. Wu, F. Zhao, and W. Mao, "View-based greenery: A three-dimensional assessment of city buildings' green visibility using floor green view index," (in English), *Landscape Urban Planning*, vol. 152, pp. 13–26, Aug. 2016, doi: 10.1016/j.landurbplan.2016.04.004.
[6] A. Van Bilsen and E. Stolk, "The potential of isovist-based visibility analysis," in *Architectural Annual 2005-2006*. Rotterdam, The Netherlands: Delft Univ. Technol, 2007, pp. 68–73.
[7] D. V. Pullar and M. E. Tidey, "Coupling 3D visualisation to qualitative assessment of built environment designs," (in English), *Landscape Urban Planning*, vol. 55, no. 1, pp. 29–40, Jun. 2001, doi: 10.1016/s0169-2046(00)00148-1.
[8] M. Llobera, "Extending GIS-based visual analysis: The concept of visualscapes," *Int. J. Geographical Inf. Sci.*, vol. 17, no. 1, pp. 25–48, Jan. 2003.
[9] J. Zhao, R. Li, and X. Wei, "Assessing the aesthetic value of traditional gardens and urban parks in China," (in English), *Proc. Inst. Civil Eng.-Urban Des. Planning*, vol. 170, no. 2, pp. 83–91, Apr. 2017, doi: 10.1680/jurdp.16.00027.
[10] S. Saeidi, S. H. Mirkarimi, M. Mohammadzadeh, A. Salmanmahiny, and C. Arrowsmith, "Assessing the visual impacts of new urban features: Coupling visibility analysis with 3D city modelling," (in English), *Geocarto Int.*, vol. 34, no. 12, pp. 1315–1331, Oct. 2019, doi: 10.1080/10106049.2018.1478891.
[11] M. O. Ruiz, "A causal analysis of error in viewsheds from USGS digital elevation models," *Trans. GIS*, vol. 2, no. 1, pp. 85–94, Oct. 1997.
[12] Z. Tong, "A viewshed approach on identifying the street spatial outline," in *Proc. 19th Int. Conf. Geoinformatics*, Jun. 2011, pp. 1–4.
[13] J. A. Barceló, "Line-of-sight and cost surface analysis using GIS," in *Pattern to Process: Methodological Investigations Into the Formation and Interpretation of Spatial Patterns in Archaeological Landscapes*, P. M. Leusen Ed. Groningen, The Netherlands: University Library Groningen, 2002.
[14] G. Zhang, P. van Oosterom, and E. Verbree, "Point cloud based visibility analysis: First experimental results," presented at the Societal Geo-Innov., Short Papers, Posters Poster Abstr. 20th Agile Conf. Geographic Inf. Sci., Wageningen, The Netherlands, 2017. [Online]. Available: https://agile-online.org/index.php/conference/proceedings/proceedings-2017
[15] Y. Zhao, B. Wu, J. Wu, S. Shu, H. Liang, M. Liu, V. Badenko, A. Fedotov, S. Yao, and B. Yu, "Mapping 3D visibility in an urban street environment from mobile LiDAR point clouds," *GIScience Remote Sens.*, vol. 57, no. 6, pp. 797–812, 2020, doi: 10.1080/15481603.2020.1804248.

[16] A. F. Chase, D. Z. Chase, J. F. Weishampel, J. B. Drake, R. L. Shrestha, K. C. Slatton, J. J. Awe, and W. E. Carter, "Airborne LiDAR, archaeology, and the ancient Maya landscape at Caracol, Belize," *J. Archaeolog. Sci.*, vol. 38, no. 2, pp. 387–398, Feb. 2011, doi: 10.1016/j.jas.2010.09.018.
[17] B. Štular, Ž. Kokalj, K. Ostir, and L. Nuninger, "Visualization of lidar-derived relief models for detection of archaeological features," *J. Archaeolog. Sci.*, vol. 39, no. 11, pp. 3354–3360, Nov. 2012, doi: 10.1016/j.jas.2012.05.029.
[18] C. Li, X. Lu, N. Zhu, Y. Lu, Y. Wu, and G. Li, "Continuously extracting section and deformation analysis for subway tunnel based on LiDAR points," (in Chinese), *Acta Geodetica et Cartographica Sinica*, vol. 44, no. 9, pp. 1056–1062, 2015. [Online]. Available: http://xb.sinomaps.com/EN/Y2015/V44/I9/1056, doi: 10.11947/j.AGCS.2015.20140632.
[19] F. Remondino, "From point cloud to surface: The modeling and visualization problem," *Int. Arch. Photogramm., Remote Sens. Spatial Inf. Sci.*, vol. 34, pp. 1–12, Feb. 2003.
[20] S. Sun and C. Salvaggio, "Aerial 3D building detection and modeling from airborne LiDAR point clouds," *IEEE J. Sel. Topics Appl. Earth Observ. Remote Sens.*, vol. 6, no. 3, pp. 1440–1449, Jun. 2013.
[21] F. Lafarge and C. Mallet, "Creating large-scale city models from 3D-point clouds: A robust approach with hybrid representation," *Int. J. Comput. Vis.*, vol. 99, no. 1, pp. 69–85, Aug. 2012.
[22] P. van Oosterom, O. Martinez-Rubi, M. Ivanova, M. Horhammer, D. Geringer, S. Ravada, T. Tijssen, M. Kodde, and R. Gonçalves, "Massive point cloud data management: Design, implementation and execution of a point cloud benchmark," *Comput. Graph.*, vol. 49, pp. 92–125, Jun. 2015.
[23] H. Liu, P. van Oosterom, M. Meijers, X. Guan, E. Verbree, and M. Horhammer, "HISTSFC: Optimization for ND massive spatial points querying," *Int. J. Database Manage. Syst.*, vol. 12, no. 3, pp. 7–28, Jun. 2020.
[24] B. Alsadik, M. Gerke, and G. Vosselman, "Visibility analysis of point cloud in close range photogrammetry," *ISPRS Ann. Photogramm., Remote Sens. Spatial Inf. Sci.*, vol. II-5, pp. 9–16, 2014.
[25] P. L. Guth, "Incorporating vegetation in viewshed and line-of-sight algorithms," in *Proc. ASPRS-Mapps Specialty Conf., Digit. Mapping, Elevation Inf.*, 2009, pp. 1–7.
[26] J. J. Murgoitio, R. Shrestha, N. F. Glenn, and L. P. Spaete, "Improved visibility calculations with tree trunk obstruction modeling from aerial LiDAR," *Int. J. Geographical Inf. Sci.*, vol. 27, no. 10, pp. 1865–1883, Oct. 2013.
[27] P. L. Guth, "Probabilistic line-of-sight with Lidar point clouds," in *Proc. ASPRS Annu. Conf.*, Sacramento, CA, USA, Mar. 2012. [Online]. Available: https://www.asprs.org/a/publications/proceedings/Sacramento2012/files/Guth.pdf
[28] Ó. Iglesias, L. Díaz-Vilariño, H. González-Jorge, and H. Lorenzo, "Interurban visibility diagnosis from point clouds," *Eur. J. Remote Sens.*, vol. 49, no. 1, pp. 673–690, Jan. 2016.
[29] R. Peters, H. Ledoux, and F. Biljecki, "Visibility analysis in a point cloud based on the medial axis transform," in *Proc. UDMV*, 2015, pp. 7–12.
[30] D. Wheatley, "Cumulative viewshed analysis: A GIS-based method for investigating intervisibility, and its archaeological application," in *Archaeology and GIS: A European Perspective*, G. Lock and Z. Stancic, Eds. London, U.K.: Routlege, 1995, pp. 171–185.
[31] AHN. *AHN: The Making of*. Accessed: Aug. 20, 2020. [Online]. Available: https://www.ahn.nl/ahn-making
[32] Wikipedia. *Naked Eye*. Accessed: Jan. 21, 2021. [Online]. Available: https://en.wikipedia.org/wiki/Naked_eye
[33] D. Girardeau-Montaut. Cloud compare-3D point cloud and mesh processing software. Open Source Project. Accessed: Sep. 29, 2016. [Online]. Available: https://www.danielgm.net/cc/
[34] "Using ArcGIS spatial analyst," Environ. Syst. Res. Inst., Redlands, CA, USA, Tech. Rep., 2001. [Online]. Available: http://downloads.esri.com/support/documentation/ao_/776Using_Spatial_Analyst.pdf
[35] Z. Tao and S. Qing, "Study on the D/H ratio of city road's environmental effect based on BIM," *J. Theor. Appl. Inf. Technol.*, vol. 49, no. 1, pp. 448–455, 2013.

GUAN-TING ZHANG received the B.S. degree in theoretical and applied mechanics from the Harbin Institute of Technology, in 2011, and the M.S. degree in landscape architecture from Southeast University, Nanjing, China, in 2014, where she is currently pursuing the Ph.D. degree in landscape architecture. Her research interests include urban studies, visual landscape, spatial analysis, and visual analysis from built environments.

EDWARD VERBREE received the M.Sc. degree in geodesy from the Delft University of Technology, in 1992. Since 1997, he has been working as an Assistant Professor with the GIS Technology Department, Delft University of Technology. His research interests include tetrahedralizations, tessellations, surface reconstruction, explorative point clouds, location awareness, and indoor positioning.

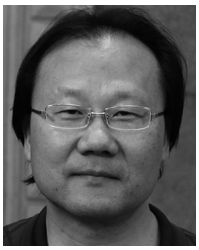

XIAO-JUN WANG received the Ph.D. degree in landscape architecture from Southeast University, Nanjing, China, in 2007. Since 2007, he has been a Professor with the Department of Landscape Architecture, School of Architecture, Southeast University. His research interests include landscape design, urban studies, the morphology, and the distribution of urban open spaces.